Am J Physiol Cell Physiol 297: C526–C536, 2009.
First published July 15, 2009; doi:10.1152/ajpcell.00572.2008.

Characterization of an epilepsy-associated variant of the human Cl^-/HCO_3^- exchanger AE3

Gonzalo L. Vilas, Danielle E. Johnson, Paul Freund, and Joseph R. Casey

Membrane Protein Research Group, Department of Physiology, University of Alberta, Edmonton, Canada

Submitted 7 November 2008; accepted in final form 11 July 2009

Vilas GL, Johnson DE, Freund P, Casey JR. Characterization of an epilepsy-associated variant of the human Cl^-/HCO_3^- exchanger AE3. *Am J Physiol Cell Physiol* 297: C526–C536, 2009. First published July 15, 2009; doi:10.1152/ajpcell.00572.2008.—Anion exchanger 3 (AE3), expressed in the brain, heart, and retina, extrudes intracellular HCO_3^- in exchange for extracellular Cl^-. The SLC4A3 gene encodes two variants of AE3, brain or full-length AE3 ($AE3_{fl}$) and cardiac AE3 (cAE3). Epilepsy is a heterogeneous group of disorders characterized by recurrent unprovoked seizures that affect about 50 million people worldwide. The AE3-A867D allele in humans has been associated with the development of IGE (IGE), which accounts for ~30% of all epilepsies. To examine the molecular basis for the association of the A867D allele with IGE, we characterized wild-type (WT) and $AE3_{fl}$-A867D in transfected human embryonic kidney (HEK)-293 cells. $AE3_{fl}$-A867D had significantly reduced transport activity relative to WT (54 ± 4%, $P < 0.01$). Differences in expression levels or the degree of protein trafficking to the plasma membrane did not account for the defect of $AE3_{fl}$-A867D. Treatment with 8-bromo-cAMP (8-Br-cAMP) increased Cl^-/HCO_3^- exchange activity of WT and $AE3_{fl}$-A867D to a similar degree, which was abolished by preincubation with the protein kinase A (PKA)-specific inhibitor H89. This indicates that PKA regulates WT and $AE3_{fl}$-A867D Cl^-/HCO_3^- exchange activity. No difference in Cl^-/HCO_3^- exchange activity was found between cultures of mixed populations of neonatal hippocampal cells from WT and slc4a3$^{-/-}$ mice. We conclude that the A867D allele is a functional (catalytic) mutant of AE3 and that the decreased activity of $AE3_{fl}$-A867D may cause changes in cell volume and abnormal intracellular pH. In the brain, these alterations may promote neuron hyperexcitability and the generation of seizures.

protein kinase A; intracellular pH

CRITICAL CELLULAR PROCESSES, including neurotransmission, phototransduction in the outer retina, ion-channel conductance, calcium homeostasis, gene expression, cell death, and contractility are affected by changes in intracellular pH (pH_i) (1, 18, 47). These examples, among others, indicate that the regulation of pH_i in eukaryotic cells is of paramount importance for the maintenance of homeostasis and the survival of organisms.

Anion exchanger 3 (AE3), a member of the solute carrier 4 (SLC4) protein family, mediates the electroneutral exchange of intracellular HCO_3^- for extracellular Cl^- across the plasma membrane. AE3 activity contributes to the regulation of pH_i, cellular volume, and Cl^- levels (15). Mammalian cells express two isoforms of AE3, brain or full-length AE3 ($AE3_{fl}$) and cardiac AE3 (cAE3) (32), generated by tissue-specific usage of alternative promoters. Human $AE3_{fl}$ and cAE3 are 1232 and 1034 amino acids long, respectively. The two AE3 variants differ only at the NH_2-terminus of their NH_2-terminal cytoplasmic domains, where the 200 amino acids of the $AE3_{fl}$ isoform are replaced by a shorter 73 amino acid sequence in cAE3. The significance of the two splicing forms has not been established, but within the retina there are cell-type specific differences in expressions of cAE3 and $AE3_{fl}$ (29).

Although AE3 is differentially expressed in excitatory tissues, the two isoforms have different distributions (30). $AE3_{fl}$ and cAE3 are expressed in the heart and retina, whereas in the brain only $AE3_{fl}$ is expressed (46). In the brain, where neuronal activity generates rapid and significant pH_i changes, $AE3_{fl}$ activity may be important for the removal of excessive intracellular HCO_3^-, thus contributing to the maintenance of normal neuronal and glial function (13, 30, 44). Neurotransmitter receptors for γ-aminobutyric acid (GABA) and glycine have intrinsic Cl^- channel activity (25). Since the degree and polarity of the response is determined by the intracellular levels of Cl^-, it has been suggested that AE3 is involved in the modulation of this response through its concentrative Cl^- activity (6).

Epilepsy is a heterogeneous group of seizure disorders that affect about 50 million people worldwide (43). Idiopathic generalized epilepsy (IGE) accounts for ~30% of all epilepsies (45). Patients affected with IGE manifest symptoms between early childhood and adolescence. IGE is characterized by recurrent and unprovoked generalized seizures that are apparently unrelated to brain lesions and/or metabolic disorders (3, 7). Genetic studies of monogenic idiopathic epilepsies identified mutations in some central nervous system ion channels (KCNJ10, KCNJ3, KCNQ2/KCNQ3, CLCN2, GABRG2, GABRA1, SCN1B, and SCN1A), suggesting that IGE presents a complex pattern of inheritance and that several genetic factors contribute to the predisposition to generalized seizures (20, 34).

The occurrence of the AE3-A867D allele in humans is associated with the development of IGE (40), yet the effect of the A867D variant on AE3 function has not been tested. AE3 knockout mice, however, display a reduced threshold for chemically induced seizures (23). Together this suggests that defects in AE3 activity may cause seizures due to abnormal regulation of neuronal pH_i and cell volume.

In this work we evaluated the functional and physiological parameters of wild-type (WT) and human $AE3_{fl}$-A867D in transiently transfected human embryonic kidney (HEK)-293 cells to investigate the potential role of $AE3_{fl}$-A867D in the development of IGE. Only $AE3_{fl}$ has been studied here, therefore, for the sake of simplicity, "AE3" as used here will imply the $AE3_{fl}$ variant. We found that WT and AE3-A867D proteins had a similar subcellular localization and were processed equally to the plasma membrane. AE3-A867D, however, had significantly reduced transport activity when compared with WT. Incubation of transiently transfected HEK-293 cells with

Address for reprint requests and other correspondence: J. R. Casey, Dept. of Physiology, Univ. of Alberta, Edmonton, Alberta T6G 2H7, Canada (e-mail: joe.casey@ualberta.ca).

protein kinase A (PKA) agonists and inhibitors showed that $AE3_{fl}$ transport activity was regulated by this kinase.

When taken together, the results indicate that the decreased transport activity of AE3-A867D may cause changes in cell volume and abnormal pH_i and Cl^- levels. In the brain these alterations may promote neuron hyperexcitability and contribute to the generation of epileptic seizures.

MATERIALS AND METHODS

Materials. Eukaryotic-expression construct for human AE3 cDNA was a gift from Dr. Seth Alper (Beth Israel Deaconess Medical Center, Boston, MA). Dual-emission, pH-sensitive green fluorescent protein cDNA (de4gfp/peGFP-N1) was a gift from Dr. Jim Remington (University of Oregon). cDNA encoding GPI-eGFP, an enhanced green fluorescent protein, containing the signal sequence of lactase-phlorizin hydrolase and a consensus *N*-glycosylation site fused to the glycosylphosphatidyl inositol (GPI)-attachment signal of lymphocyte-function-associated-antigen 3 (28), was a gift from Dr. Todd Alexander (University of Alberta). Oligonucleotides were from Integrated DNA Technologies (Coralville, IA). Restriction enzymes were from New England Biolabs (Ipswich, MA). Pfx DNA polymerase, Dulbecco's modified Eagle's medium (DMEM), neurobasal medium, fetal bovine serum, calf serum, penicillin-streptomycin-glutamine, and BCECF-AM were from Invitrogen (Carlsbad, CA). Cell culture dishes were from Corning (Corning, NY). Glass coverslips were from Fisher Scientific (Ottawa, ON, Canada). Complete protease inhibitor was from Roche Applied Science (Indianapolis, IN). BCA Protein Assay Kit and immobilized streptavidin resin were from Pierce (Rockford, IL). H89, 8-bromo-cAMP (8-Br-cAMP), nigericin, and poly-L-Lysine were from Sigma-Aldrich (Oakville, ON, Canada). Mouse anti-glyceraldehyde-3-phosphate dehydrogenase (GAPDH) and horseradish peroxidase (HRP)-conjugated donkey anti-rabbit IgG were from Santa Cruz Biotechnology (Santa Cruz, CA). Affinity purified rabbit anti-human AE3 antibodies, generated using the polypeptide NFDEGQDEYNEC corresponding to amino acids 1216 to 1227 located at the cytoplasmic carboxy-terminal domain of the protein, were prepared by Genscript (Piscataway, NJ) and called AE3ct. Alexa-coupled antibodies and Prolong Antifade Gold, Solution were from Molecular Probes (Carlsbad, CA). HRP-conjugated donkey anti-mouse IgG and protein A Sepharose CL-4B were from GE Healthcare Bio-Sciences (Piscattaway, NJ).

DNA constructs. Human AE3-A867D cDNA was constructed using the mega-primer mutagenesis strategy (41). The first round of PCR used the forward primer 5′-*gcgcgtggtggagaccatgattgtg*-3′ and the reverse mutagenic primer 5′-*cagaccagcatccagggacc*-3′ thus generating the substitution of the Ala codon 867 for Asp. For the second round of amplification, the product from the first PCR reaction was used as forward mega primer and 5′-*gcgcgtactcatcctggccatcctc*-3′ as reverse primer. The second round PCR product was cloned back into human AE3 cDNA using *Eag*I and *Nsi*I restriction sites, and the new construct was then sequenced to confirm the presence of the desired mutation.

Tissue culture. WT AE3, AE3-A867D, or pcDNA were expressed alone or coexpressed with deGFP4 in a 4:1 molar ratio, by transient transfection of HEK-293 cells, using the calcium phosphate method (38). Cells were grown at 37°C in an air-CO_2 (19:1) environment in DMEM, supplemented with 5% (vol/vol) fetal bovine serum, 5% (vol/vol) calf serum, and 1% (vol/vol) penicillin-streptomycin-glutamine. All experiments involving transfected cells were carried out 40 to 48 h posttransfection.

Isolation of hippocampal neurons. Hippocampi were dissected from the brains of 15.5 d WT and slc4a3$^{-/-}$ mice mouse embryos (19 WT and 14 ae3$^{-/-}$) (17). slc4a3$^{-/-}$ mice, whose characterization and method of genotyping have been previously reported (1), were obtained from Dr. Gary Shull (University of Cincinnati). Samples were incubated for 25 min at 37°C in Hanks' buffered saline solution (in mM: 5.3 KCl, 137.9 NaCl, 4.6 D-glucose, 0.4 KH_2PO_4, 0.3 Na_2HPO_4, and 4.2 $NaHCO_3^-$, pH 7.3), containing 0.5% (vol/vol) trypsin. After incubation neurobasal medium, supplemented with B27 supplement, 200 mM L-glutamine and 10,000 U/ml penicillin-streptomycin were added, and samples were mixed for 1–2 min by inversion. Samples were centrifuged at 600 *g* for 5 min. Supernatant was aspirated and the samples were further triturated 10 times with a Pasteur pipette in fresh neurobasal medium. Samples were left to settle for 5 min, and the supernatant was transferred to a new tube. Samples were centrifuged at 150 *g* for 5 min. Pellets were resuspended in 4 ml medium. Cells were counted, and $\sim 1 \times 10^6$ cells/ml were plated onto 25-mm poly-L-lysine-coated coverslips. Cultures were incubated at 37°C in an air-CO_2 (19:1) environment and assayed for Cl^-/HCO_3^- activity 16–26 h after isolation.

Fluorimeter-based measurements of cytosolic pH. HEK-293 cells, grown and transfected on 11 × 7.5 mm coverslips, were incubated at 37°C for 30 min in DMEM, containing 3 μM of the pH-sensitive dye, BCECF-AM, and mounted in a fluorescence cuvette. BCECF fluorescence changes were monitored in a PTI RCR fluorimeter (Photon Technologies International) at excitation wavelengths 502.5/440 nm and emission wavelength 528.7 nm. The remaining cells were washed with 4°C PBS (in mM: 140 NaCl, 3 KCl, 6.5 Na_2HPO_3, 1.5 KH_2PO_3, pH 7.4), lysed in IPB buffer (1% NP40, 5 mM EDTA, 0.15 M NaCl, 0.5% deoxycholate, and 10 mM Tris·HCl, pH 7.5), containing Complete Protease Inhibitor. Protein content was determined using the BCA method.

Photometric measurements of cytosolic pH. HEK-293 cells transiently transfected with WT AE3, AE3-A867D, deGFP4, or pcDNA constructs or hippocampal neurons from WT or ae3$^{-/-}$ mice were grown on 25-mm circular poly-L-lysine-coated glass coverslips. Coverslips were rinsed with 37°C Ringer solution (HEK-293 cells) or incubated at 37°C for 30 min in DMEM, containing 3 μM of the pH-sensitive dye BCECF-AM (hippocampal cultures) and mounted in a 35-mm diameter Attofluor Cell Chamber (Molecular Probes). The chamber holds a custom-built insert, reducing the internal diameter to 13 mm. The chamber was then placed on a Leica DMIRB inverted microscope equipped with a PTI D-104 microscope photometer. The light source, connected to the microscope via a fiber optic cable, was a 75-W xenon arc lamp in a PTI DeltaScan excitation monochromator equipped with a chopper to enable dual excitation wavelength measurements. Excitation wavelengths were set to 400 nm (when monitoring deGFP4) or 440 and 502.5 nm (when monitoring BCECF). Wavelengths of emitted light were selected with a cube mounted in the microscope containing a 425-nm beam splitter, and a cube mounted in the photometer containing a 485-nm beam splitter, a 445- to 475-nm emission filter, and a 495- to 525-nm emission filter (deGFP4) or a cube mounted in the microscope containing a 515-nm beam splitter and a 522.5- to 547.5-nm emission filter (BCECF).

Cl^-/HCO_3^- exchange activity assays. Transfected HEK-293 cells, either mounted on the microscope stage, as described above, or mounted in a fluorescence cuvette, were perfused alternately with Ringer buffer (in mM: 5 glucose, 5 potassium gluconate, 1 calcium gluconate, 1 $MgSO_4$, 2.4 NaH_2PO_4, 25 $NaHCO_3$, and 10 HEPES, pH 7.4), containing either 140 mM NaCl or 140 mM sodium gluconate. Both buffers were continuously bubbled with 5% CO_2 (balance air) and adjusted to pH 7.4 with NaOH. Fluorescence of deGFP4 or BCECF was monitored at the excitation and emission wavelengths described above. For deGFP4-transfected HEK-293 cells, three to five transfected cells were selected for pH_i measurements on the basis of their green fluorescence. Fluorescence data were converted into pH_i by calibration using the nigericin-high potassium method (48) with reference pH values near 6.5, 7.0, and 7.5. Cl^-/HCO_3^- exchange rates were calculated by linear regression of the initial rate of pH_i change during perfusion with Cl^--free buffer. For BCECF experiments, normalized AE3 exchange activity was calculated as Cl^-/HCO_3^- exchange rates/total AE3 protein present in 50 μg of cell lysate as

quantified on immunoblots subjected to densitometry. Data are presented as percentage of WT AE3 and corrected for background exchange activity of empty vector-transfected cells.

Coverslips containing hippocampal neurons from WT or slc4a3$^{-/-}$ embryonic mice previously incubated with 3 μM BCECF-AM were mounted on the microscope stage, perfused, and analyzed as described above. Approximately 20 cells were selected for pH_i measurements.

Measurement of intrinsic buffer capacity and proton flux. Intracellular buffer capacity measurements were made by the ammonium chloride pulse method (33). Briefly, HEK-293 cells were transiently transfected with WT or A867D cDNA AE3 as described above, and 2 days posttransfection the cells were loaded with BCECF-AM. Coverslips were mounted in a fluorescence cuvette and allowed to equilibrate in Ringer buffer without $NaHCO_3$. Cells were consecutively perfused for 200 s with $NaHCO_3$-free Ringer buffer containing 20, 10, 5, 1, and 0 mM NH_4Cl. Fluorescence changes were recorded and the data were converted into pH_i using the nigericin-high potassium method as described above. The NH_4Cl intracellular concentration ($[NH_4Cl]_i$) was calculated using the Henderson-Hasselbalch equation, and the intrinsic buffer capacity (β_i) was then calculated as $\Delta[NH_4Cl]_i/\Delta pH_i$ (42, 47). Total buffer capacity of the cells (β_{Total}) was calculated as $\beta_{Total} = \beta_i + \beta_{CO_2}$, where $\beta_{CO_2} = 2.3\ [HCO_3^-]$ (33). Proton equivalent flux (J_{H^+}) was calculated as: $J_{H^+} = (\Delta pH_i/dt) \times \beta_{Total}$.

Immunoblot analysis. Samples were prepared in 2× SDS-PAGE sample buffer [10% (vol/vol) glycerol, 2% (wt/vol) SDS, 0.5% (wt/vol) bromophenol blue, 75 mM Tris, pH 6.8], containing complete protease inhibitor. Before analysis, samples were made to 1% (vol/vol) 2-mercaptoethanol and heated for 4 min at 65°C, and insoluble material was removed by centrifugation at 16,000 *g* for 10 min. Samples were then resolved by SDS-PAGE on 7.5% (wt/vol) acrylamide gels (31). Proteins were electrotransferred onto Immobilon-P PVDF membranes (Millipore, MA) for 1 h at a constant current of 400 mA. After transfer, membranes were rinsed in TBS (0.15 M NaCl, 50 mM Tris·HCl, pH 7.5) and incubated with 5% (wt/vol) skim milk TBS-T [0.1% (vol/vol) Tween-20, 0.15 M NaCl, 50 mM Tris·HCl, pH 7.5] for 1 h at room temperature with gentle rocking to block nonspecific binding. Membranes were then incubated for 16 h at 4°C with gentle rocking in the presence of either rabbit anti-human AE3ct, mouse anti-GAPDH at a 1:2,500 or 1:2,000 dilution in 5% skim milk TBS-T, respectively. After successive washes with TBS and TBS-T, the membranes were incubated with a 1:5,000 dilution of the appropriate HRP-conjugated secondary antibodies in 5% skim milk TBS-T for 1 h at room temperature and further washed with TBS and TBS-T. Proteins were detected using Western Lightning Chemiluminescence Reagent Plus (PerkinElmer) and visualized using a Kodak Image Station 440CF (Kodak, NY). Quantitative densitometric analyses were performed using Kodak Molecular Imaging Software v4.0.3 (Kodak, NY).

Cell surface processing assay. HEK-293 cells were transiently transfected with cDNAs encoding WT, AE3-A867D, or pcDNA 3.1 (empty vector) as described above. Forty to forty eight hours posttransfection, cells were rinsed with 4°C PBS, washed with 4°C borate buffer (mM: 154 NaCl, 7.2 KCl, 1.8 $CaCl_2$, and 10 boric acid, pH 9.0) and then incubated for 30 min at 4°C in borate buffer containing Sulfo-NHS-SS-Biotin (0.5 mg/ml, Pierce, IL). After being washed three times with 4°C quenching buffer (192 mM glycine, 25 mM Tris, pH 8.3), cells were solubilized 20 min on ice in 500 μl of IPB, containing complete protease inhibitor. Cell lysates were centrifuged for 20 min at 13,200 *g* and the supernatants recovered. For each sample, half of the supernatant was retained for later SDS-PAGE analysis (total protein, T). The remaining half of the supernatants were combined with 50 μl of a 50% slurry of immobilized streptavidin resin in PBS and incubated 16 h at 4°C with gentle rotation. Samples were centrifuged for 2 min at 8,000 *g*, and the supernatant was collected (unbound protein, U). The T and U fractions of each sample were analyzed by SDS-PAGE and immunoblotting as described above. After densitometric quantitation of the corresponding bands, the percentage of biotinylated protein was calculated as $(T - U)/T \times 100\%$.

Confocal microscopy. Cells grown on 22 × 22 mm poly-L-lysine-coated coverslips were individually transfected with WT, AE3-A867D cDNAs, or empty vector or cotransfected with GPI-eGFP as described above. Two days posttransfection cells were washed twice with PBS, fixed with 3.5% paraformaldehyde, 1 mM $CaCl_2$, and 1 mM $MgCl_2$ in PBS, pH 7.4, for 20 min, washed twice with PBS, and then quenched with 50 mM NH_4Cl for 10 min. Fixed cells were permeabilized with 0.1% Triton X-100 in PBS for 1 min at room temperature, followed by a 30-min block with 0.2% (wt/vol) gelatin in PBS. After blocking was completed, coverslips were incubated for 1 h in a humidified chamber in the presence of rabbit anti-human AE3ct and mouse monoclonal anti-calnexin antibodies at 1:1,000 and 1:500 dilutions in 0.2% (wt/vol) gelatin in PBS, respectively. After three washes with 0.2% (wt/vol) gelatin in PBS, coverslips were further incubated for 1 h in a dark humidified chamber in the presence of goat anti-rabbit IgG conjugated with Alexa Fluor 594 and chicken anti-mouse IgG conjugated with Alexa Fluor 488 at 1:1,000 dilutions in 0.2% (wt/vol) gelatin in PBS to detect AE3 and calnexin, respectively. Finally, coverslips were washed three times with 0.2% (wt/vol) gelatin in PBS, rinsed twice with PBS, and mounted in Prolong Antifade Gold Solution containing the DNA-specific fluorescent dye 4′,6-diamidino-2-phenylindole. Images were obtained with a Zeiss LSM 510 laser scanning confocal microscope (Carl Zeiss MicroImaging), mounted on an Axiovert 100M controller with a ×63 (numerical aperature 1.4) lens.

Colocalization studies. Confocal images, obtained as described above, were analyzed with Volocity software (Improvision, Waltham, MA).

Statistical analysis. Analysis was performed using Prism software (Graphpad). Groups were compared with one-way ANOVA and paired *t*-test with $P < 0.05$ considered significant.

RESULTS

The AE3 A867D sequence variant is associated with IGE, yet the functional effects of this change, whether it is a polymorphism or a functional mutation, have not been assessed. To determine the effects of this mutation, we compared the Cl^-/HCO_3^- exchange activity of WT and mutant human AE3. HEK-293 cells were transiently transfected with either WT or AE3-A867D cDNA and subjected to Cl^-/HCO_3^- exchange assays. Cells were loaded with the pH-sensitive dye BCECF-AM and alternatively perfused with Cl^--containing and Cl^--free (where equimolar membrane impermeant sodium gluconate replaces NaCl) buffers in a fluorescence cuvette (47). When perfused with Cl^--free buffer, AE3 mediates the efflux of cytoplasmic Cl^- in exchange for extracellular HCO_3^-, which increases pH_i, as measured by an increase in fluorescence. Figure 1*A* illustrates the typical anion-exchange data obtained for empty vector AE3-A867D and WT AE3. Steady-state pH_i in Cl^--containing medium was 7.19 ± 0.03, 7.20 ± 0.004, and 7.20 ± 0.03 pH units for vector, AE3-A867D, and WT AE3, respectively (Supplemental Fig. 1*A*). Transport rates were determined from the initial alkalinization rate upon switching from Cl^--containing to Cl^--free medium. Intrinsic buffer capacity (β_i) of vector A867D and WT AE3-transfected HEK-293 cells at pH_i 7.20 were 10 ± 1, 10 ± 0.4, and 10 ± 1 mM/pH, respectively (Supplemental Fig. 1*B*). Flux of proton equivalents (in units of $mM \cdot min^{-1}$) was then calculated as $dpH/dT \cdot \beta_{total}$. Cl^-/HCO_3^- exchange rate of AE3-A867D transfected cells was significantly slower ($P < 0.05$) than WT AE3-transfected cells (5 ± 1 and 11 ± 2 mM/min, respec-

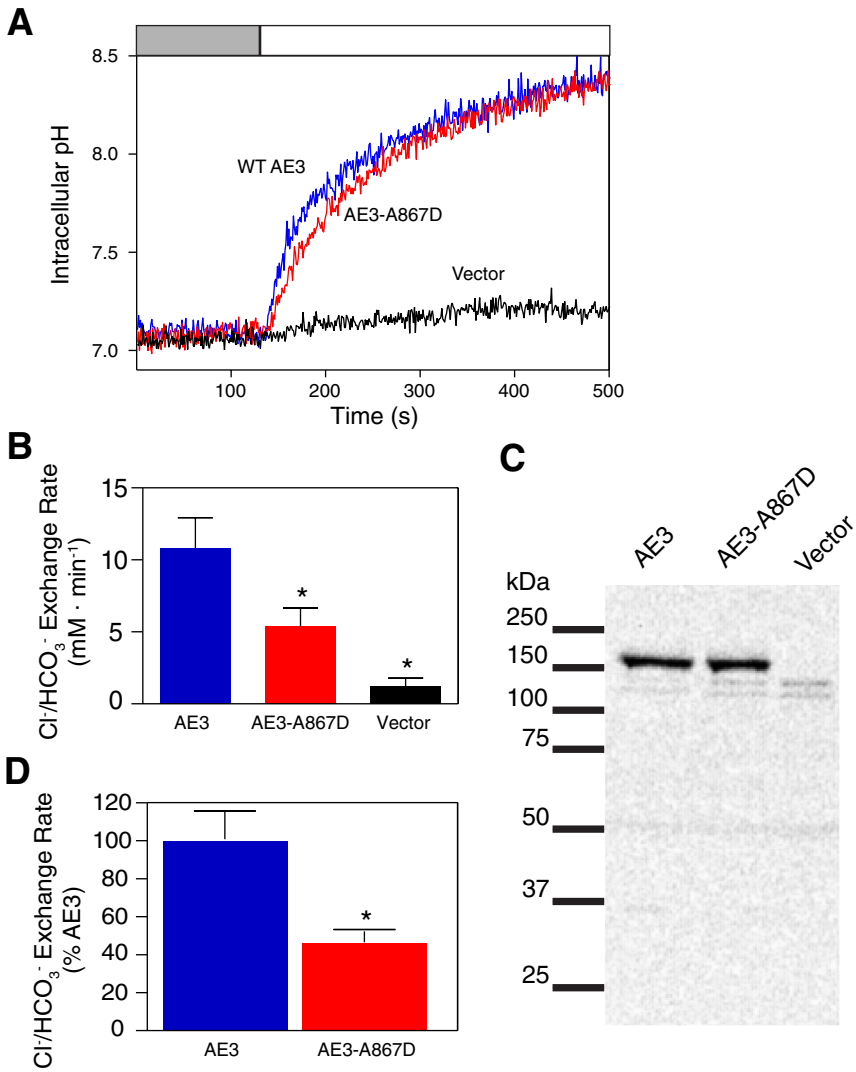

Fig. 1. *A*: Cl^-/HCO_3^- exchange activity of wild-type (WT) and anion exchanger 3 (AE3)-A867D measured in whole fields of cells. Human embryonic kidney (HEK)-293 cells, grown on glass coverslips and transfected with empty vector or cDNA encoding either human WT AE3 or AE3-A867D, were incubated with the pH-sensitive dye BCECF-AM. Coverslips were then placed in a fluorescence cuvette and perfused alternately with Cl^--containing (shaded bar) and Cl^--free (open bar) Ringer buffer. Fluorescence changes, associated with variations in intracellular pH (pH_i), were monitored in a fluorimeter, using λ_{ex} = 440 and 502.5 nm and λ_{em} = 528.7 nm. Blue, red, and black traces represent results from WT, AE3-A867D, and empty vector, respectively. *B*: mean Cl^-/HCO_3^- exchange activity calculated by linear regression of the initial rate of pH_i change during perfusion with Cl^--free buffer. *C*: cell lysates, prepared from cells used in Cl^-/HCO_3^- exchange assays, were subjected to immunoblotting and probed with AE3ct antibody, which recognizes the COOH-terminal tail of AE3 protein. *D*: transport activities corrected for activity of vector-transfected cells and normalized for AE3 protein expression. Values are expressed as percentage of WT AE3. Error bars represent SE ($n \geq 5$). *Significant difference ($P < 0.05$) compared with WT AE3 exchange activity.

tively) (Fig. 1*B*). Both rates were significantly faster than found for vector-alone transfected cells (1.2 ± 0.6 mM/min). Intrinsic buffer capacities and the anion-exchange activity for AE3 presented here agree with those previously reported (12, 47).

To correct for differences in the level of expression of the two AE3 variants, cells used in each transport assay were subjected to immunoblotting and probed with anti-human AE3 (AE3ct) antibody (Fig. 1*C*). This is the first report characterizing the AE3ct antibody, generated in rabbits immunized with a peptide, corresponding to the COOH-terminal residues of human AE3 (1216–1227). A strong band is present at the expected molecular weight of AE3 in cells transfected with WT and AE3-A867D cDNAs but not in vector-alone transfected cells (Fig. 1*C*). Lower molecular weight bands are present in both AE3- and vector-transfected cells, indicating that they represent nonspecific cross-reactive bands.

To compare the absolute transport turnover of the two proteins, the background anion exchange activity of vector-transfected cells was subtracted from those of AE3-A867D and WT AE3-transfected cells. The resulting transport rates were normalized for the amount of AE3 expressed in the cells, detected by immunoblotting, and quantified by densitometry. AE3-A867D had a significantly lower relative Cl^-/HCO_3^- exchange activity (47 ± 13%, $P < 0.05$) when compared with WT AE3 (Fig. 1*D*).

AE3-A867D transport activity was also assessed in a small group of cells monitored on a microscope stage. HEK-293 cells were transiently cotransfected with WT AE3, AE3-A867D, or pcDNA3.1 and cDNA encoding the dual-emission, pH-sensitive green fluorescent protein deGFP4 (21) at a 4:1 molar ratio. Importantly, deGFP4 fluorescence is virtually Cl^- insensitive (26), which makes it ideal for monitoring pH_i changes associated with Cl^-/HCO_3^- exchange. Fluorescence of three to five transfected cells (identified by their green fluorescence) was monitored by photometry as the cells were perfused alternately with Cl^--containing and Cl^--free Ringer buffers, as described above. At the end of each experiment, fluorescence values were calibrated to pH using the nigericin-high potassium technique, and Cl^-/HCO_3^- exchange activity was calculated by the linear regression of the initial rate of pH_i change during perfusion with Cl^--free buffer. Representative traces of Cl^-/HCO_3^- exchange activity mediated by WT AE3, AE3-A867D, and vector-alone transfected cells are shown in Fig. 2*A*. AE3-A867D had a significantly lower activity than WT (8 ± 1 and 15 ± 1 mM/min, respectively) (Fig. 2*B*). Further calculations revealed that AE3-A867D has a relative activity of 54 ± 4%

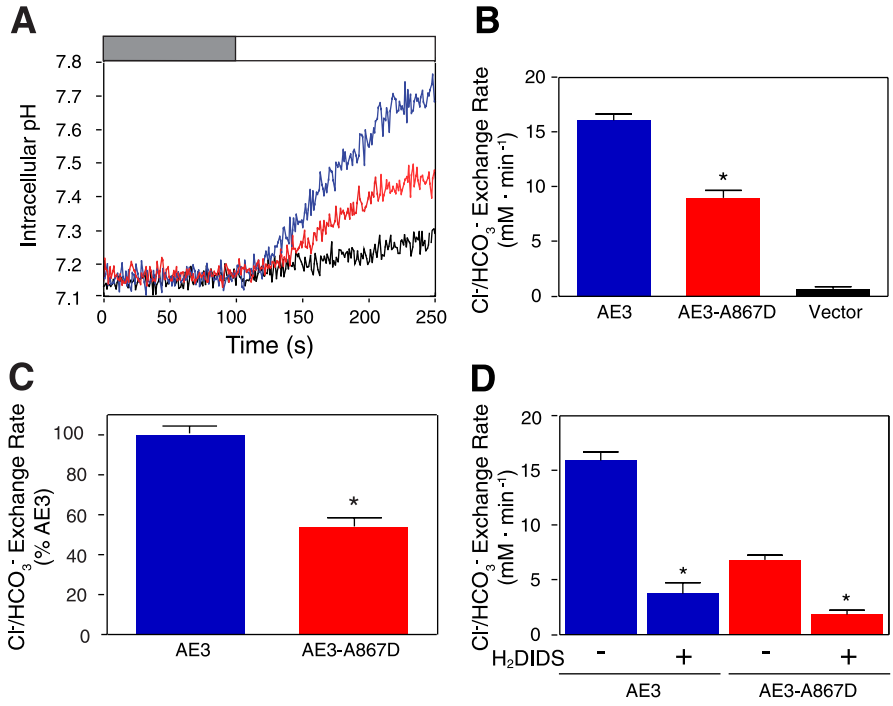

Fig. 2. Cl^-/HCO_3^- exchange activity of WT and AE3-A867D measured by microscopic photometry. *A*: HEK-293 cells were transiently cotransfected with deGFP4 cDNA and WT AE3, AE3-A867D, or empty vector in a 1:4 molar ratio. deGFP4 fluorescence was monitored at λ_{ex} = 400 nm and λ_{em} = 460 and 510 nm. Cells were perfused alternately with Cl^--containing (shaded bar) and Cl^--free (open bar) Ringer buffer. At the end of each experiment fluorescence values for pH-sensitive deGFP were calibrated to pH_i via the nigericin-high potassium technique. Blue, red, and black traces represent results from WT AE3, AE3-A867D, and vector-transfected cells, respectively. *B*: mean Cl^-/HCO_3^- exchange activity calculated by linear regression of the initial rate of pH_i change during perfusion with Cl^--free buffer. *C*: transport activities, corrected for activity of vector-transfected cells. Error bars represent SE (n = 3). *Significant difference ($P < 0.01$) when compared with WT AE3. *D*: HEK-293 cells, transfected with WT AE3 or AE3-A867D, were subjected to Cl^-/HCO_3^- exchange assays in the absence (−) and then presence (+) of 200 μM 4,4′-diisothiocyano-1,2-diphenylethane-2,2′-disulfonic acid (H_2DIDS). Between the two assays cells were incubated for 3 min in Cl^--containing Ringer buffer with 200 μM H_2DIDS. Rates of Cl^-/HCO_3^- exchange were determined from the rate of alkalinization upon switching to Cl^--free Ringer buffer. Error bars represent SE (n = 3). *Significant difference ($P < 0.01$) when compared with rate in the absence of H_2DIDS.

when compared with WT (Fig. 2*C*). After incubation with the disulfonic stilbene bicarbonate transport inhibitor H_2DIDS (200 μM), AE3-A867D and WT AE3 retained 27 ± 10% and 24 ± 11% of their original activities, respectively (Fig. 2*D*). Thus the transport activity of both AE3 proteins was sensitive to H_2DIDS. Assays of Cl^-/HCO_3^- activity measured in BCECF-loaded fields of cells (Fig. 1) reported a lower absolute rate of transport than using pH-sensitive deGFP in small groups of cells (Fig. 2). This may reflect the low sample chamber volume (200 μl) in the microscope experiments, resulting in rapid exchange between Cl^--containing and Cl^--free solutions, driving more rapid transport. In both assays, however, the transport activity of AE3-A867D was essentially half that of WT AE3.

To investigate the pathophysiological importance of an impaired AE3 activity, we analyzed Cl^-/HCO_3^- exchange in mixed hippocampal neuron/glia cultures isolated from WT and ae3$^{-/-}$ mice at developmental stage E15.5 (5, 23, 27). Sixteen to twenty-four hours after isolation, the cultures were incubated with the pH-sensitive dye BCECF-AM. An average of 20 cells were selected per experiment to ensure the presence of neurons in the sample. Cells were perfused alternately with Cl^--containing and Cl^--free Ringer buffers to initiate Cl^-/HCO_3^- exchange (Supplemental Fig. 2*A*). There was no significant difference in dpH/dT between the WT and ae3$^{-/-}$ hippocampal neuron-glia cultures upon switching to Cl^--free buffer (0.016 ± 0.002 and 0.018 ± 0.005 pH U/min, respectively) (Supplemental Fig. 2*B*). Furthermore, no significant difference in the baseline pH_i of WT and ae3$^{-/-}$ cultured hippocampal cells (7.26 ± 0.01 and 7.27 ± 0.02 pH units, respectively) were detected (Supplemental Fig. 2*C*). These results indicate that, under our experimental conditions, there is no significant Cl^-/HCO_3^- exchange activity evident in either neuron population, in agreement with previous findings, indicating that AE3 may not be functional in fetal neurons (37).

Mutations in membrane proteins often result in misfolding that may lead to decreased activity, impairment of biogenesis, endoplasmic reticulum retention, and abolished or decreased expression at its target membrane(s) (4, 22). Since anion-exchange assays only measure the activity of proteins at the plasma membrane, reduced cell surface expression levels of functional AE3 can result in an apparent lower anion exchange activity. To test whether the AE3-A867D mutation affects AE3 membrane processing, we quantified the amount of protein present at the cell surface by cell surface biotinylation assays of HEK-293 cells transiently transfected with empty vector, AE3-A867D, or WT AE3. Two days posttransfection the cells were labelled with the membrane-impermeant biotinylation reagent Sulfo-NHS-SS-biotin and then lysed with IPB buffer. After solubilization, half of the total lysate (T) was retained and the remainder was incubated with streptavidin-agarose resin and centrifuged to remove biotinylated protein. Equal volumes of biotin-free (U) and total (T) lysates were separated by SDS-PAGE. The presence of AE3 and the endogenous cytosolic protein GAPDH (negative control) was determined by immunoblot (Fig. 3*A*). Densitometric analysis revealed that 37 ± 5% of WT, 32 ± 2% of AE3-A867D, and 8 ± 2% of GAPDH were accessible to the biotinylation reagent, implying plasma membrane localization (Fig. 3*B*). The presence of a low level of biotinylated GAPDH may reflect the fact that some of the cells were damaged during the experiment therefore exposing cytoplasmic proteins to the labeling reagent. Thus the GAPDH plasma membrane localization value (8 ± 2%) represents the background value for the assay. The AE3 cell surface processing percentage presented in this work further confirms the values previously reported by our laboratory for this protein (47). The difference between WT and AE3-A867D cell surface processing was statistically insignificant, thus suggesting that the plasma membrane expression is similar for both proteins.

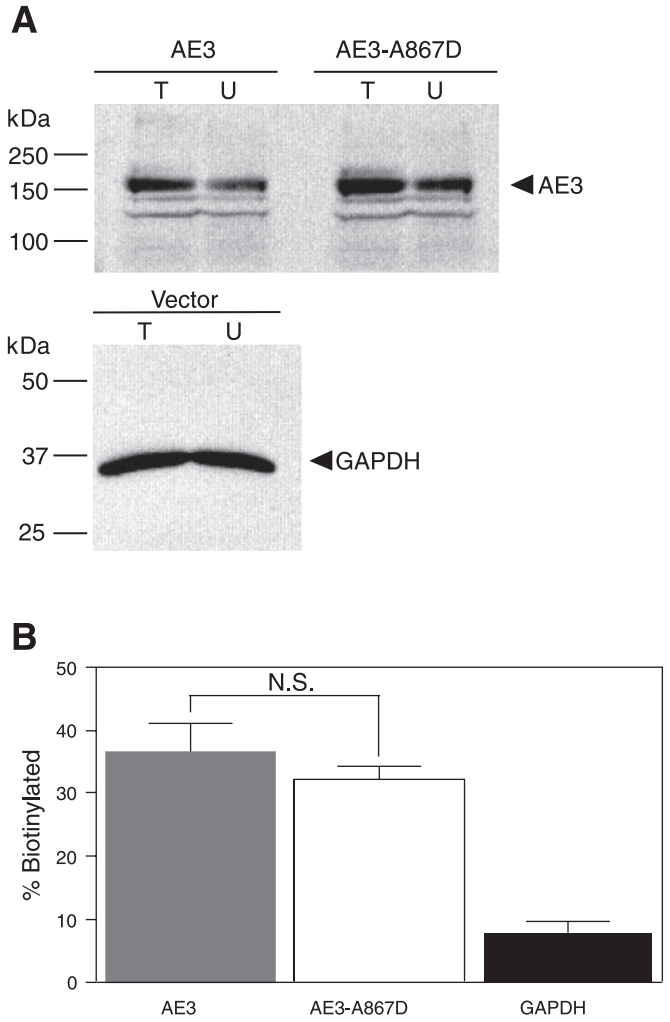

Fig. 3. Assay of cell surface localization of human WT and AE3-A867D. HEK-293 cells were transiently transfected with cDNA encoding either WT or AE3-A867D or empty vector. Cells were labeled with Sulfo-NHS-SS-biotin and lysed, and half of the lysate was incubated with streptavidin-agarose resin to remove biotinylated proteins. *A*: equal fractions of total lysate (T) and unbound supernatant fraction (U) were separated by SDS-PAGE. Immunoblots were probed with AE3ct anti-AE3 and anti-GAPDH antibodies. *B*: fraction of protein labeled by the membrane-impermeant biotinylation reagent (representing protein at the cell surface), as calculated by densitometry, is shown. Error bars represent SE ($n = 6$). *t*-Test revealed no significant difference (NS) between the two AE3 proteins.

To investigate further whether the A867D mutation affects AE3 biogenesis, we compared the subcellular localization of WT and AE3-A867D expressed in transiently transfected HEK-293 cells using confocal microscopy. WT and AE3-A867D had similar subcellular distribution patterns, with the majority of the protein present in the endoplasmic reticulum and some protein located at the plasma membrane, as judged by the extent of signal overlapping with the endoplasmic reticulum-specific marker calnexin (Fig. 4*A*) and the plasma membrane-targeted GPI-eGFP protein (Fig. 4*B*), respectively. Colocalization of the markers with AE3 was quantified, using Pearson's coefficient (Fig. 4*C*). The degree of colocalization found for vector-alone transfected cells represents nonspecific signal and therefore the threshold above which there is significant overlap between the fluorescent signals. Framed in this way, both AE3 WT and AE3-A867D colocalize with calnexin and GPI-eGFP, indicating respectively localization of AE3 in the endoplasmic reticulum and at the plasma membrane. Colocalization analysis, however, revealed no significant difference in the localization of WT and AE3-A867D (Fig. 4*C*). Consistent with the biotinylation data (Fig. 3), these results indicate that at a steady state the majority of synthesized AE3 is present in the endoplasmic reticulum and that the mutation does not greatly affect the biogenesis and subcellular localization of exogenously expressed AE3-A867D. Furthermore, this result supports our previous finding that only a fraction of the synthesized protein reaches the plasma membrane. Taken together, the results presented so far indicate that differences in baseline pH_i, intrinsic buffer capacity, cell surface processing, and subcellular localization do not explain the reduced anion exchange activity of AE3-A867D.

The occurrence of the A867D AE3 allele in humans is associated with the development of IGE (40). Moreover, AE3 knockout mice display a reduced threshold for chemically induced seizures (23). Metabotropic glutamate receptors (mGluRs) are monomeric G protein-coupled receptors that contain a large NH_2-terminal extracellular tail that harbors the glutamate binding site (14). These receptors transduce extracellular signals via the second messenger cAMP and participate in various adaptive and pathological neurological events, including synaptic plasticity, excitotoxicity, and the pathogenesis of epilepsy (11, 35). We thus considered whether cAMP-coupled signaling events might differentially regulate AE3 and the A867D variant. In support of the notion, protein kinase-specific eukaryotic protein phosphorylation prediction algorithms (8) indicated the presence of five PKA consensus phosphorylation motifs predicted to have ≥60% probability to act as a PKA site (data not shown) in the AE3 amino-terminal cytosolic domain.

We therefore characterized the effect of PKA on AE3 transport activity. Transport activity of HEK-293 cells transiently transfected with empty vector, AE3-A867D, or WT AE3 is significantly increased after incubation with the membrane-permeant cAMP analog and PKA agonist 8-Br-cAMP (100 μM for 10 min) and decreases when preincubated with the PKA inhibitor H89 (10 μM) for 5 min and then further incubated for 10 min in the presence of both H89 and 8-Br-cAMP (Fig. 5*A*).

To compare the effect that these treatments have on the transport activity of the two proteins, AE3-A867D and WT AE3 anion exchange activities were corrected for background Cl^-/HCO_3^- exchange activity of empty vector-transfected cells. The resulting transport rates were normalized for the amount of AE3 expressed in the cells, which was detected by immunoblotting and quantified by densitometry. 8-Br-cAMP significantly increased both WT and AE3-A867D anion exchange activity by 26 ± 11% and 36 ± 9%, respectively, compared with corresponding untreated transfected cells (Fig. 5*B*).

Treatment with H89 not only abolished the stimulatory effects of 8-Br-cAMP but significantly decreased transport activity for both WT and AE3-A867D by 33 ± 13% and 19 ± 9%, respectively, when compared with untreated transfected cells, suggesting that there is basal cAMP-stimulation of AE3 transport activity in HEK-293 cells. As a control, anion exchange activity of transfected cells was measured after two successive Cl^--free buffer pulses in the absence of agonist, and

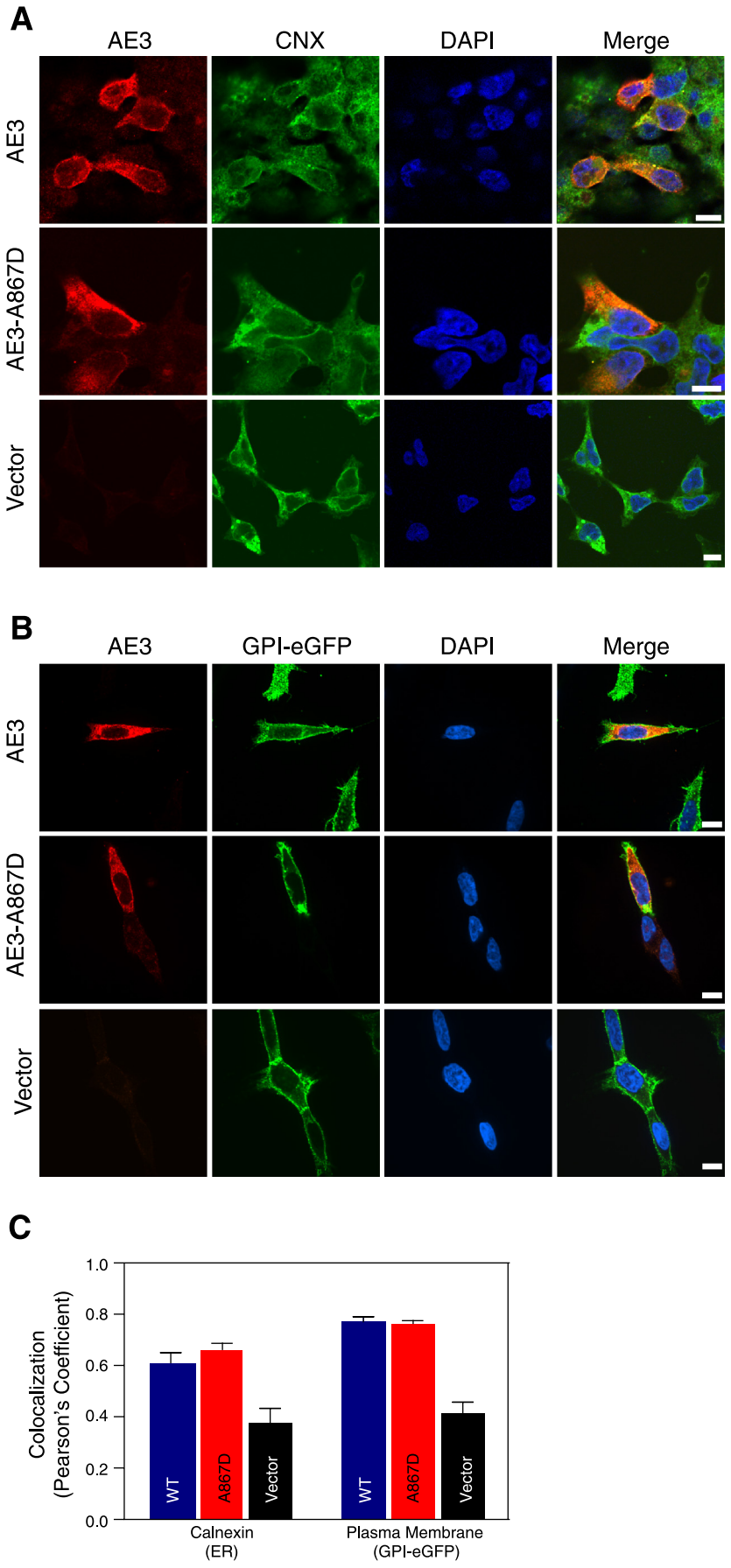

Fig. 4. Subcellular localization of WT AE3 and AE3-A867D. HEK-293 cells individually transfected with WT or AE3-A867D cDNAs or empty vector (*A*) or cotransfected with GPI-eGFP (*B*) were grown on glass coverslips and processed for confocal immunofluorescence microscopy. AE3 was detected using rabbit anti-AE3 antibody and goat anti-rabbit IgG conjugated with Alexa Fluor 594 (red). Endoplasmic reticulum (ER) marker calnexin (CNX) was detected with a mouse anti-CNX monoclonal antibody and chicken anti-mouse IgG conjugated with Alexa Fluor 488 (green). Green fluorescence of the plasma membrane marker GPI-eGFP was detected directly. Nuclei were detected with DAPI (blue), as indicated. The merged images are presented in the far right-hand column. Scale bars represent 10 μm. *C*: Pearson's linear correlation coefficient overlap between florescence signals from ER marker CNX and plasma membrane-associated GPI-eGFP with WT (blue bars) and AE3-A867D (red bars) was measured using Volocity software. Black bars represent nonspecific values calculated for vector-alone transfected cells. Error bars represent SE ($n \geq 6$). *t*-Test revealed no significant difference in the degree of colocalization between the two AE3 proteins and the markers.

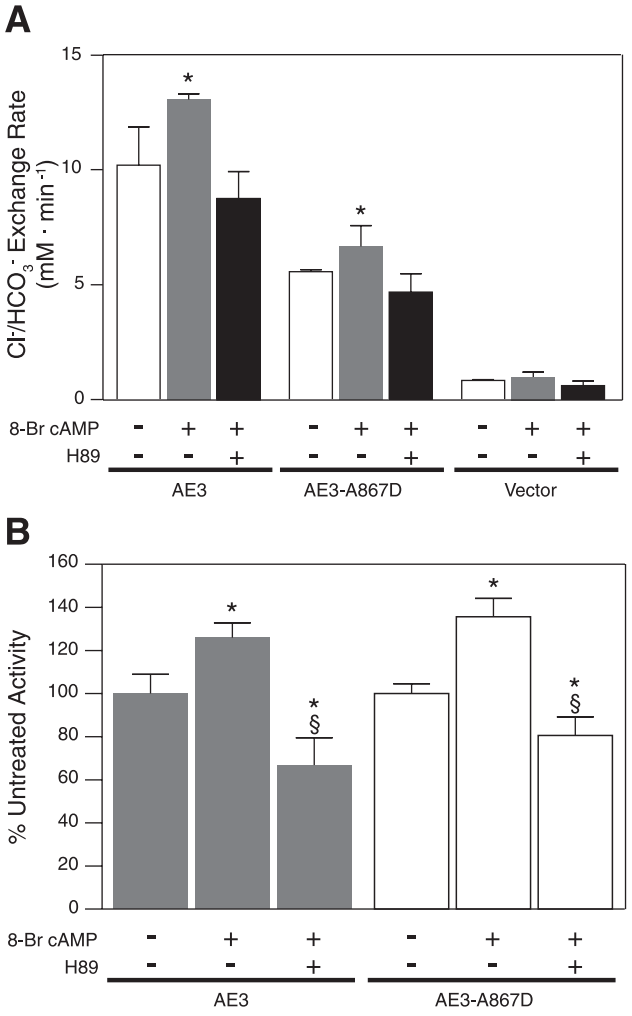

Fig. 5. Regulation of human AE3 by cAMP-coupled pathways. HEK-293 cells were grown on glass coverslips, individually transfected with cDNA encoding WT AE3, AE3-A867D, or empty vector. Cells were loaded with the pH-sensitive dye BCECF-AM and coverslips were then placed in a fluorescence cuvette. Cells were perfused alternately with Cl^--containing and Cl^--free Ringer buffer and either incubated in Cl^--free Ringer buffer with the protein kinase A (PKA) agonist 8-Br-cAMP (100 μM) for 10 min, preincubated with the PKA inhibitor H89 (10 μM) for 5 min, and further incubated for 10 min with 8-Br-cAMP (100 μM), or left untreated for 15 min followed by a repeat of the Ringer buffer perfusion cycle in the presence of the compounds. During the experiment, changes in intracellular pH (pH_i)-associated fluorescence were monitored in a fluorimeter, using λ_{ex} = 440 nm and 502.5 nm and λ_{em} = 528.7 nm. *A*: anion exchange activity of cells untreated (open bars), treated with PKA agonist 8-Br-cAMP (shaded bars) or treated with 8-Br-cAMP and the specific PKA inhibitor H89 (solid bars). *B*: transport activities, corrected for activity of vector-transfected cells and normalized for AE3 protein expression. Error bars represent SE (n = 4). § and *Statistical difference ($P < 0.05$) when compared with untreated and H89 + 8-Br-cAMP-treated exchange activity, respectively.

no significant differences were found in the two rates (100 ± 4% vs. 110 ± 20% for the first and second pulses, respectively).

Finally, we investigated whether the stimulation of transport activity observed upon treatment with 8-Br-cAMP was associated with an increase in the cell surface expression of AE3. HEK-293 cells, transiently transfected with AE3-A867D or WT AE3, were incubated with vehicle or 100 μM of the PKA agonist 8-Br-cAMP for 10 min, and the amount of protein present at the cell surface was quantified by cell surface biotinylation assays. Treatment with 8-Br-cAMP did not significantly increase the amount of either AE3-A867D or WT AE3 present at the plasma membrane (Supplemental Fig. 3), suggesting that cAMP does not alter AE3 activity through insertion of vesicular-localized AE3 into the plasma membrane. These results indicate that both WT and AE3-A867D transport activities increase similarly when intracellular cAMP levels are increased and that PKA is involved in this activation.

Taken together, the results presented here indicate that AE3-A867D has about half the Cl^-/HCO_3^- exchange activity of WT AE3. Differences in cell surface processing, subcellular localization, and sensitivity to cAMP-coupled signaling pathways do not explain the decreased activity of AE3-A867D.

DISCUSSION

In this work we examined the transport activity, subcellular localization, and PKA-mediated regulation of AE3-A867D, an allele associated with development of IGE in humans (40). The results presented here reveal that the AE3-A867D allele represents a functional mutation, which results in a reduction in transport activity by about one-half relative to WT AE3. Decreased Cl^-/HCO_3^- exchange activity of AE3-A867D is not caused by defects in protein expression level, cell surface processing, or subcellular localization, as assessed respectively by quantitative immunoblots, cell surface biotinylation assays, and confocal immunofluorescence. AE3 transport activity was increased by PKA, as shown by the stimulatory effects of 8-Br-cAMP, which were suppressed by the PKA inhibitor H89. The similar effect of PKA on WT and AE3-A867D indicates that differences in regulation by the cAMP-coupled signaling pathway do not explain the association of the allele with IGE seizures. We conclude that reduction of AE3 Cl^-/HCO_3^- exchange activity by 50% is sufficient to promote increased susceptibility to epileptic seizures in humans.

In an attempt to understand the role that AE3 plays in seizure sensitivity in vivo, we measured the Cl^-/HCO_3^- exchange of mixed hippocampal neuron-glia cultures isolated from WT and $ae3^{-/-}$ mice at developmental stage E15.5. We found no significant differences in either transport activity or baseline pH_i, consistent with previous measurements of rat fetal hippocampal neurons, which did not display active Cl^-/HCO_3^- exchange (37). Thus, whereas AE3 may have an important role in adult brain, the role is not manifested in fetal brain cells. These data suggest that despite the presence of AE3 message in the cells (23), AE3 does not play an active role in the pH regulation of neurons in the developing brain. Cl^-/HCO_3^- exchange studies performed in hippocampal slices of adult $ae3^{-/-}$ mice, however, showed that AE3 is the dominant anion exchanger in the hippocampus (23). Failure to detect Cl^-/HCO_3^- exchange in these assays may reflect the use of a mixed population of cells, in which the AE3-expressing cells were a subpopulation whose activity could not be detected on the backdrop of other cells. Alternatively, AE3 expression may have been downregulated during the 16-h interval between the time the cells were isolated from the mice and the time Cl^-/HCO_3^- exchange assays were performed. This time period was, unfortunately, the minimum period required to allow the cells to set down on the tissue culture dishes.

Humans carrying the A867D allele would likely be heterozygous. Since AE3-A867D has half the activity of WT

AE3, 75% of AE3 Cl^-/HCO_3^- exchange activity from AE3 should remain. Thus the increase of epilepsy associated with AE3-A867D arises from only an expected loss of only 25% of AE3 transport activity. Is any insight available from $ae3^{+/-}$ mice? Despite the finding that AE3 is the major Cl^-/HCO_3^- exchanger in adult mice brain (23), $ae3^{-/-}$ and $ae3^{+/-}$ mice were fertile, developed normally, and were indistinguishably behaviorally and anatomically from their $ae3^{+/+}$ littermates (1, 23). Closer examination revealed no obvious morphological changes or degeneration in the brain of the $ae3^{-/-}$ animals (23). Disruption of the slc4a3 gene in these animals, however, resulted in higher sensitivity to seizure-inducing agents, inner retinal defects, and late onset photoreceptor death (1, 23). The $ae3^{+/-}$ mice had more than a twofold reduction in AE3 protein expression in their retinas (1), suggesting that loss of one allele in some way affects accumulation of AE3 by the unaffected allele, or that cells expressing AE3 protein decrease in abundance. Unfortunately, there has been no report of the sensitivity of $ae3^{+/-}$ mice to seizures.

Interestingly, in AE3-A867D, the mutated amino acid residue is present in the third extracellular loop of the protein, located between transmembrane segments 5 and 6 on the basis of sequence alignment with AE1, whose topology has been extensively studied (52). On the basis of this location, residues in this loop may interact with AE3 substrates on route to the transmembrane ion translocation pore. Substitution of the nonpolar amino acid Ala^{867} for the acidic Asp could constitute an electrostatic hindrance to the negatively charged Cl^- and HCO_3^- moving toward the AE3 anion translocation channel. Of interest, the human AE3-A867H variant is not associated with epilepsy (40). This may reflect a tolerance for positive charge at the A867 position. Alternatively, histidine at this position may be in an environment that disfavors side chain protonation, meaning that the residue conserves the noncharged character of native A867.

As with other Cl^-/HCO_3^- exchangers (2, 10, 47), the cytoplasmic domain of AE3 proteins probably interacts with the membrane domain to regulate activity. Computational studies predicted five Ser-containing sequences likely to be phosphorylated by PKA (phosphorylation probability $\geq$60%). Among these, a site encompassing Ser 553 was predicted to be phosphorylated by PKA with the second highest degree of confidence (78%). PKA activity is dependent on the level of cAMP in the cell. Interestingly, an important group of neuronal receptors, the metabotropic glutamate receptors (mGluRs) involved in the pathogenesis of epilepsy, are G protein-coupled receptors and transduce extracellular cues via the second messenger cAMP (11, 35). We therefore studied whether the activity of both WT and AE3-A867D was modulated by PKA. The results obtained using PKA agonists and inhibitors on transiently transfected cells indicate that the activity of both AE3 isoforms is significantly increased by PKA and decreased in the presence of the PKA-specific inhibitor H89. These experiments indicate that the activity of AE3 is modulated by intracellular cAMP levels, in line with observations that PKA regulates the activities of the Na^+-dependent and Na^+-independent Cl^-/HCO_3^- exchangers in adult rat CA1 neurons (9). This is, however, the first report on the regulation of AE3 by PKA or even cAMP. Interestingly, the extent of activation and inhibition of Cl^-/HCO_3^- transport elicited by 8-Br-cAMP and H89 on cells transfected with either WT or AE3-A867D is very similar, suggesting that the Ala to Asp mutation does not affect the activity modulation mediated by the cytoplasmic domain but rather decreases the overall transport capacity of the protein.

How could a reduction of AE3 Cl^-/HCO_3^- exchange activity underlie some cases of IGE? AE3 has a broad expression pattern in the mouse brain with a particularly strong presence in the stratum pyramidale of the hippocampal CA3 region (23). This region contains the cell bodies of the pyramidal neurons, which are the principal excitatory neurons of the hippocampus and are considered to be the "pacemaker" of this structure (49). Much of the synchronous bursting activity, associated with intervals between seizures, appears to be generated in CA3 (19, 49). AE3 Cl^-/HCO_3^- exchange activity reduces cytosolic HCO_3^- levels with a concomitant intracellular increase in Cl^- concentration. If AE3 transport occurs in a confined space or area with low perfusion, a depletion of extracellular Cl^- and an increase of HCO_3^- will occur. As a consequence of these direct effects, AE3-mediated efflux of HCO_3^- from the cytosol will acidify the cell and alkalinize the extracellular space. Decreased AE3 activity would result in altered intra- and extracellular pH as well as Cl^- levels. In turn this could alter the ligand-binding properties of receptors in the extracellular milieu and/or signal transduction processes in the cytosol. Our observation that the A867D mutation reduces AE3 activity is consistent with the increased sensitivity to chemically induced seizures seen in $AE3^{-/-}$ mice (23).

Can changes of cytosolic or extracellular Cl^-, HCO_3^- or pH cause epilepsy? Interestingly, mice null for the KCC2 neuron-specific $K^+/2Cl^-$ cotransporter display neuronal hyperexcitability (50) and increased susceptibility to seizures (51). KCC2 normally functions to maintain low cytosolic Cl^- levels in an electroneutral manner. Since glycine and GABA receptors both conduct Cl^-, this shifts their reversal potentials to more negative values (50). Analogously, reduced Cl^- accumulating AE3 activity (as in the A867D mutant) would reduce the driving force for the two Cl^--conducting receptors mentioned above, but in the opposite direction, since a reduced AE3 activity will decrease the amount of intracellular Cl^-. A role for pH regulation in control of epilepsy is suggested by the spontaneous mouse mutant of the alkalinizing Na^+/H^+ exchanger (NHE1), which displays slow wave epilepsy; this could, however be secondary to brain structural changes, rather than a result of alkalinizing capacity (16). Finally, mice with a targeted gene disruption of the electroneutral Na^+/HCO_3^- cotransporter SLC4A10 (36), a relative of AE3 (SLC4A3), have markedly reduced sensitivity to chemically induced seizures (24). Thus disruption of HCO_3^--accumulating SLC4A10 function reduces seizures, whereas loss of AE3's HCO_3^- efflux function promotes them. Since SLC4A10 does not, under physiological conditions, have a Na^+-driven Cl^-/HCO_3^- exchange activity but mediates an electroneutral Na^+/HCO_3^- cotransport, the neuronal $[Cl^-]_i$ levels are likely to remain unaffected (36). Together this implies that the acidifying HCO_3^- efflux capacity of AE3 is the function that is needed to help suppress epileptic seizures (24, 50).

Epilepsy affects about 50 million people worldwide and nearly 30% of these patients are affected by IGE (43, 45). Epileptic seizures occur when neurons keep firing instead of transmitting electrical pulses in a controlled manner. This disturbance in brain electrical excitability can result in invol-

untary spasmodic muscle contractions and unconsciousness (43). Neuronal activity and metabolism generate important changes in intracellular and extracellular pH (13). Many ion channels are sensitive to pH, therefore, the tight modulation and control of pH_i is necessary for proper brain function, which is maintained by several proteins (23). Among these is the Cl^-/HCO_3^- exchanger AE3 (46).

Genome-linkage analysis mapped a susceptibility locus for IGE to the chromosomal region containing the AE3 gene (39). Subsequently, a high frequency of the A867D allele variant was found in patients with IGE (40). It was unclear, however, whether the AE3-A867D alteration or changes in a nearby gene increased risk of IGE. Our findings, together with the characterization of $ae3^{-/-}$ mice as epilepsy prone (23), suggest a possible explanation for the correlation between the occurrence of the AE3-A867D allele and the development of IGE. Our data show that AE3-A867D has a catalytic defect relative to WT AE3, resulting in a twofold reduction in Cl^-/HCO_3^- exchange activity. The sensitivity of the neuronal activity to intracellular $[Cl^-]$ and pH^i suggest that reduced AE3 activity contributes to promoting neuron hyperexcitability and the generation of seizures.

ACKNOWLEDGMENTS

We thank Alysa Tennese for the preparation of the mouse hippocampal neuronal cultures.

GRANTS

G. L. Vilas, D. E. Johnson, and J. R. Casey are respectively a postdoctoral fellow, graduate student, and Scientist supported by the Alberta Heritage Foundation for Medical Research.

REFERENCES

1. **Alvarez BV, Gilmour G, Mema SC, Shull GE, Casey JR, Sauvé Y.** Blindness results from deficiency in AE3 chloride/bicarbonate exchanger. *PloS ONE* 2: e839, 2007.
2. **Alvarez BV, Vilas GL, Casey JR.** Metabolon disruption: a mechanism that regulates bicarbonate transport. *EMBO J* 24: 2499–2511, 2005.
3. **Andermann F, Berkovic S.** The idiopathic generalized epilepsies across life. *Suppl Clin Neurophysiol* 57: 408–414, 2004.
4. **Anelli T, Sitia R.** Protein quality control in the early secretory pathway. *EMBO J* 27: 315–327, 2008.
5. **Azevedo FA, Carvalho LR, Grinberg LT, Farfel JM, Ferretti RE, Leite RE, Jacob Filho W, Lent R, Herculano-Houzel S.** Equal numbers of neuronal and nonneuronal cells make the human brain an isometrically scaled-up primate brain. *J Comp Neurol* 513: 532–541, 2009.
6. **Becker M, Nothwang HG, Friauf E.** Differential expression pattern of chloride transporters NCC, NKCC2, KCC1, KCC3, KCC4, and AE3 in the developing rat auditory brainstem. *Cell Tissue Res* 312: 155–165, 2003.
7. **Beghi M, Beghi E, Cornaggia CM, Gobbi G.** Idiopathic generalized epilepsies of adolescence. *Epilepsia* 47, *Suppl* 2: 107–110, 2006.
8. **Blom N, Sicheritz-Ponten T, Gupta R, Gammeltoft S, Brunak S.** Prediction of post-translational glycosylation and phosphorylation of proteins from the amino acid sequence. *Proteomics* 4: 1633–1649, 2004.
9. **Brett CL, Kelly T, Sheldon C, Church J.** Regulation of Cl^--HCO_3^- exchangers by cAMP-dependent protein kinase in adult rat hippocampal CA1 neurons. *J Physiol* 545: 837–853, 2002.
10. **Camillion de Hurtado MC, Alvarez BV, Ennis IL, Cingolani HE.** Stimulation of myocardial Na^+-independent Cl^--HCO_3^- exchanger by angiotensin II is mediated by endogenous endothelin. *Circ Res* 86: 622–627, 2000.
11. **Catania MV, D'Antoni S, Bonaccorso CM, Aronica E, Bear MF, Nicoletti F.** Group I metabotropic glutamate receptors: a role in neurodevelopmental disorders? *Mol Neurobiol* 35: 298–307, 2007.
12. **Ch'en FF, Dilworth E, Swietach P, Goddard RS, and Vaughan-Jones RD.** Temperature dependence of Na^+-H^+ dxchange, Na^+-HCO_3^- Co-transport, intracellular buffering and intracellular pH in guinea-pig ventricular myocytes. *J Physiol* 15: 15, 2003.
13. **Chesler M, Kaila K.** Modulation of pH by neuronal activity. *Trends Neurosci* 15: 396–402, 1992.
14. **Conn PJ, Pin JP.** Pharmacology and functions of metabotropic glutamate receptors. *Annu Rev Pharmacol Toxicol* 37: 205–237, 1997.
15. **Cordat E, Casey JR.** Bicarbonate transport in cell physiology and disease. *Biochem J* 417: 423–439, 2009.
16. **Cox GA, Lutz CM, Yang CL, Biemesderfer D, Bronson RT, Fu A, Aronson PS, Noebels JL, Frankel WN.** Sodium/hydrogen exchanger gene defect in slow-wave epilepsy mutant mice. *Cell* 91: 139–148, 1997.
17. **Dotti CG, Sullivan CA, Banker GA.** The establishment of polarity by hippocampal neurons in culture. *J Neurosci* 8: 1454–1468, 1988.
18. **Edwards RH.** The neurotransmitter cycle and quantal size. *Neuron* 55: 835–858, 2007.
19. **Engel J Jr.** Progress in epilepsy: reducing the treatment gap and the promise of biomarkers. *Curr Opin Neurol* 21: 150–154, 2008.
20. **Gurnett CA, Hedera P.** New ideas in epilepsy genetics: novel epilepsy genes, copy number alterations, and gene regulation. *Arch Neurol* 64: 324–328, 2007.
21. **Hanson GT, McAnaney TB, Park ES, Rendell ME, Yarbrough DK, Chu S, Xi L, Boxer SG, Montrose MH, Remington SJ.** Green fluorescent protein variants as ratiometric dual emission pH sensors. 1. Structural characterization and preliminary application. *Biochemistry* 41: 15477–15488, 2002.
22. **Hebert DN, Molinari M.** In and out of the ER: protein folding, quality control, degradation, and related human diseases. *Physiol Rev* 87: 1377–1408, 2007.
23. **Hentschke M, Wiemann M, Hentschke S, Kurth I, Hermans-Borgmeyer I, Seidenbecher T, Jentsch TJ, Gal A, Hubner CA.** Mice with a targeted disruption of the Cl^-/HCO_3^- exchanger AE3 display a reduced seizure threshold. *Mol Cell Biol* 26: 182–191, 2006.
24. **Jacobs S, Ruusuvuori E, Sipila ST, Haapanen A, Damkier HH, Kurth I, Hentschke M, Schweizer M, Rudhard Y, Laatikainen LM, Tyynela J, Praetorius J, Voipio J, Hubner CA.** Mice with targeted Slc4a10 gene disruption have small brain ventricles and show reduced neuronal excitability. *Proc Natl Acad Sci USA* 105: 311–316, 2008.
25. **Jin JY, Chen WY, Zhou CX, Chen ZH, Yu-Ying Y, Ni Y, Chan HC, Shi QX.** Activation of GABAA receptor/Cl^- channel and capacitation in rat spermatozoa: HCO_3^- and Cl^- are essential. *Syst Biol Reprod Med* 55: 97–108, 2009.
26. **Johnson DE, Casey JR.** pH micro-environments associated with transport activity of the erythrocyte membrane Cl^-/HCO_3^- exchanger. *FASEB J* 22: 759.710, 2008.
27. **Kaech S, Banker G.** Culturing hippocampal neurons. *Nat Protoc* 1: 2406–2415, 2006.
28. **Keller P, Toomre D, Diaz E, White J, Simons K.** Multicolour imaging of post-Golgi sorting and trafficking in live cells. *Nat Cell Biol* 3: 140–149, 2001.
29. **Kobayashi S, Morgans CW, Casey JR, Kopito RR.** AE3 anion exchanger isoforms in the vertebrate retina: developmental regulation and differential expression in neurons and glia. *J Neurosci* 14: 6266–6279, 1994.
30. **Kopito RR, Lee BS, Simmons DM, Lindsey AE, Morgans CW, Schneider K.** Regulation of intracellular pH by a neuronal homolog of the erythrocyte anion exchanger. *Cell* 59: 927–937, 1989.
31. **Laemmli UK.** Cleavage of structural proteins during assembly of the head of bacteriophage T4. *Nature* 227: 680–685, 1970.
32. **Linn SC, Kudrycki KE, Shull GE.** The predicted translation product of a cardiac AE3 mRNA contains an N-terminus distinct from that of the brain AE3 Cl^-/HCO_3^- exchanger. *J Biol Chem* 267: 7927–7935, 1992.
33. **Loiselle FB, Casey JR.** Measurement of cell pH. *Methods Mol Biol* 227: 259–280, 2003.
34. **Lucarini N, Verrotti A, Napolioni V, Bosco G, Curatolo P.** Genetic polymorphisms and idiopathic generalized epilepsies. *Pediatr Neurol* 37: 157–164, 2007.
35. **McNamara JO, Huang YZ, Leonard AS.** Molecular signaling mechanisms underlying epileptogenesis. *Sci STKE* 2006: re12, 2006.
36. **Parker MD, Musa-Aziz R, Rojas JD, Choi I, Daly CM, Boron WF.** Characterization of human SLC4A10 as an electroneutral Na/HCO_3 co-transporter (NBCn2) with Cl^- self-exchange activity. *J Biol Chem* 283: 12777–12788, 2008.

37. **Raley-Susman KM, Sapolsky RM, Kopito RR.** Cl^-/HCO_3^- exchange function differs in adult and fetal rat hippocampal neurons. *Brain Res* 614: 308–314, 1993.
38. **Ruetz S, Lindsey AE, Kopito RR.** Function and biosynthesis of erythroid and nonerythroid anion exchangers. *Soc Gen Physiologists Series* 48: 193–200, 1993.
39. **Sander T, Schulz H, Saar K, Gennaro E, Riggio MC, Bianchi A, Zara F, Luna D, Bulteau C, Kaminska A, Ville D, Cieuta C, Picard F, Prud'homme JF, Bate L, Sundquist A, Gardiner RM, Janssen GA, de Haan GJ, Kasteleijn-Nolst-Trenite DG, Bader A, Lindhout D, Riess O, Wienker TF, Janz D, and Reis A.** Genome search for susceptibility loci of common idiopathic generalised epilepsies. *Hum Mol Genet* 9: 1465–1472, 2000.
40. **Sander T, Toliat MR, Heils A, Leschik G, Becker C, Ruschendorf F, Rohde K, Mundlos S, Nurnberg P.** Association of the 867Asp variant of the human anion exchanger 3 gene with common subtypes of IGE. *Epilepsy Res* 51: 249–255, 2002.
41. **Sarkar G, Sommer SS.** The megaprimer method of site-directed mutagenesis. *Biotechniques* 8: 404–407, 1990.
42. **Silva NL, Wang H, Harris CV, Singh D, Fliegel L.** Characterization of the Na^+/H^+ exchanger in human choriocarcinoma (BeWo) cells. *Pflügers Arch* 433: 792–802, 1997.
43. **Smith PE.** The bare essentials: epilepsy. *Pract Neurol* 8: 195–202, 2008.
44. **Staley KJ, Proctor WR.** Modulation of mammalian dendritic GABA(A) receptor function by the kinetics of Cl^- and HCO_3^- transport. *J Physiol* 519: 693–712, 1999.
45. **Steinlein OK.** Genetics and epilepsy. *Dialogues Clin Neurosci* 10: 29–38, 2008.
46. **Sterling D, Casey JR.** Bicarbonate transport proteins. *Biochem Cell Biol* 80: 483–497, 2002.
47. **Sterling D, Casey JR.** Transport activity of AE3 chloride/bicarbonate anion-exchange proteins and their regulation by intracellular pH. *Biochem J* 344: 221–229, 1999.
48. **Thomas JA, Buchsbaum RN, Zimniak A, Racker E.** Intracellular pH measurements in Ehrlich ascites tumor cells utilizing spectroscopic probes generated in situ. *Biochemistry* 18: 2210–2218, 1979.
49. **Wiebe S.** Epilepsy: A comprehensive textbook on CD-ROM. *BMJ* 320: 810A, 2000.
50. **Zhu L, Lovinger D, Delpire E.** Cortical neurons lacking KCC2 expression show impaired regulation of intracellular chloride. *J Neurophysiol* 93: 1557–1568, 2005.
51. **Zhu L, Polley N, Mathews GC, Delpire E.** NKCC1 and KCC2 prevent hyperexcitability in the mouse hippocampus. *Epilepsy Res* 79: 201–212, 2008.
52. **Zhu Q, Lee DWK, Casey JR.** Novel topology in C-terminal region of the human plasma membrane anion exchanger AE1. *J Biol Chem* 278: 3112–3120, 2003.